Accepted Manuscript

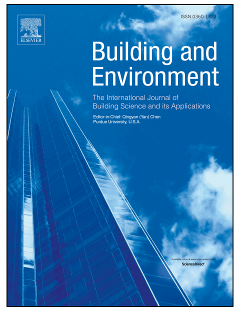

Methodology for airflow rate measurements in a naturally ventilated mock-up animal building with side and ridge vents

P. Van Overbeke, G. De Vogeleer, L.B. Mendes, E. Brusselman, P. Demeyer, J.G. Pieters

PII: S0360-1323(16)30194-9

DOI: 10.1016/j.buildenv.2016.05.036

Reference: BAE 4510

To appear in: *Building and Environment*

Received Date: 23 February 2016

Revised Date: 26 May 2016

Accepted Date: 27 May 2016

Methodology for airflow rate measurements in a naturally ventilated mock-up animal building with side and ridge vents

P. Van Overbeke[1,2], G. De Vogeleer[1,2], L.B. Mendes[1,§], E. Brusselman[1], P. Demeyer[1,*], J.G. Pieters[2]

[1]Technology & Food Unit, Institute for Agricultural and Fisheries Research (ILVO), B. Van Gansberghelaan 115, 9820 Merelbeke, Belgium,

[2] Department of Biosystems Engineering, Ghent University, Coupure links 653, 9000 Ghent, Belgium

[§]Present affiliation: Ecosystems Services and Management / Mitigation of Air Pollution and Greenhouse Gases, International Institute for Applied Systems Analysis, Schlossplatz 1, A-2361 Laxenburg, Austria

[*]Corresponding author: Peter.Demeyer@ilvo.vlaanderen.be, tel: 003292722764

Abstract:

Currently there exists no generally accepted reference technique to measure the ventilation rate through naturally ventilated (NV) vents. This has an impact on the reliability of airflow rate control techniques and emission rate measurements in NV animal houses. As an attempt to address this issue a NV test facility was built to develop new airflow rate measurement techniques for both side wall and ridge vents. Three set-ups were used that differed in vent configuration, i.e. one cross ventilated set-up and two ridge ventilated set-ups with different vent sizes.

The airflow through the side vents was measured with a technique based on an automatic traverse movement of a 3D ultrasonic anemometer. In the ridge, 7 static 2D ultrasonic anemometers were installed. The methods were validated by applying the air mass conservation principle, i.e. the inflow rates must equal the outflow rates.

The calculated in- and outflow rates agreed within (5 ± 8)%, (8 ± 5)% and (-9 ± 7)% for the three different set-ups respectively, over a large range of wind incidence angles. It was found that the side vent configuration was of large importance for the distribution of the airflow rates through the vents. The ridge proved to be a constant outlet, whilst side vents could change from outlet to inlet depending on the wind incidence angle. The range of wind incidence angles in which this transition occurred could be clearly visualised.

1 Introduction

In Europe, agriculture is considered to be responsible for the contribution of 93% and 18% of ammonia and methane emissions, respectively [1]. The negative effects on the environment such as acidification, eutrophication and ozone pollution have brought about international legislation [2,3].

In Flanders and the Netherlands the quantity of this contribution to pollution has an effect on the authorisation to renew environmental permits. This entailed a large need for effective abatement techniques with reliable and proven reduction potentials applicable in animal houses. For the quantification of both the emission rates and reduction potentials accurate measuring techniques are essential.

In general the emission rate of a gas is estimated by multiplying the ventilation rate by the pollutant's concentration at the outlet opening (corrected for background) [4]. In mechanically ventilated animal houses the ventilation rate is relatively easily determined by using e.g. free running impellers [5,6]. Furthermore, the outlet opening is fixed, delivering a clear and unchanging measuring location for the gas concentrations. However, at European level virtually all dairy farms and a significant part of pig houses are naturally ventilated. Determining the emission rate in such buildings is considerably more complex as both the ventilation rate and the outlet locations are unknown or at least constantly changing throughout time [7]. This variability is mainly due to the fluctuating outdoor conditions such as wind direction, wind speed and temperature differences which result in a complex interaction between wind and stack effect [8].

Many different approaches exist to study the ventilation rate from naturally ventilated buildings, i.e. wind tunnel set-ups [9–13], modelling [14,15], CFD [16–18] and full scale measurements [19–21]. For full scale measurements the tracer gas technique, more in particular the constant injection rate method, is the most commonly used method. Other tracer techniques such as the constant concentration method and tracer gas decay method exist but are less applicable in naturally ventilated buildings [22]. In the constant injection rate technique a tracer gas is injected into the animal house at a fixed and known rate. The relation between injection rate and the measured concentrations of the tracer gives an estimate of the ventilation rate [23]. Although the application of such techniques is widespread it has some important disadvantages. It should be noted that accurately measuring a gas concentration at a certain location in itself is not the main challenge as many reliable gas analysing systems exist. However, it is finding a representative location for these measurements that poses problems as the indoor climate in a naturally ventilated animal house is often heterogeneous [18]. Hence, choosing a less representative location could lead to large errors [24]. Furthermore, due to the constantly changing flow patterns the optimal measuring location, i.e. at the outlets, will vary as the inlet vents can become outlets and vice versa resulting from changes in outdoor conditions. Inaccuracies for tracer gas tests have been reported to vary from 10% to 230% [6]. Other techniques, including tracer gas techniques have been discussed in detail by Ogink et al [22]. where it is stated that none of the existing techniques can be considered as a reference technique. Therefore, the reduction potential of the existing and new emission abatement techniques are uncertain and prone to discussion [22,25,26]. It is thus clear that to construct an unambiguous regulatory framework aiding farmers, constructers, legislators and researchers, a reference measuring technique for the emission rate in naturally ventilated animal houses is necessary.

The basis for an accurate determination of the emission rate lies within a reliable technique to accurately measure the ventilation rate. Van Overbeke et al. [27] developed a new measuring method for the ventilation rate in naturally ventilated buildings. The method is based on a 3D ultrasonic anemometer that automatically traverses the whole of the ventilation opening through the aid of a linear guidance system. Driven by a programmable logical controller (PLC), the sensor stopped at pre-defined locations in the ventilation opening to measure the air velocity after which it moved to the next location. The data collected at these different locations were then combined to determine the airflow rate. This method was validated against a reference technique for mechanical ventilation [28,29] as no reference for naturally ventilated flows exists. In those studies, the ability of the method to accurately measure heterogeneous velocity profiles was evidenced. Subsequently, a naturally ventilated test facility was built where the methods' ability of coping with the continuously changing velocity profiles in the vents was examined [27]. Although satisfying results were obtained, the method has so far been applied to small openings only (0.5 m × 1.0 m), in a cross ventilated section of the test facility. However, cross ventilation alone rarely occurs in naturally ventilated buildings, which usually feature a ridge vent. The ridge plays an important role in the airflow patterns and might significantly affect the ventilation rate as well [30,31].

Therefore the objective of this research was to examine the applicability of the previously developed method in situations more representative of commercial animal houses, i.e. cross and ridge ventilation. The method was applied to and validated on larger vent openings (0.5 × 3.0 m) and an additional measuring technique for the ventilation rate through the ridge was developed and validated. Also, the in- and outlet character of all vents was examined. The longer term objective of this research is to obtain a test facility in which the velocity profiles in each vent are characterised under a large range of wind incidence angles and speeds through the aid of the method developed in this paper. This test facility could then be an important benchmark in the development of accurate ventilation rate measurement techniques transferable to commercial naturally ventilated animal houses.

2 Materials and Methods

2.1 Test facility

A full scale section of a pig house was built at the Institute for Agricultural and Fisheries Research in Merelbeke, Belgium (+50° 58' 38.56'' N, +3° 46' 45.68'' E). This building, further referred to as the test facility (See Fig. 1), was also used by Van Overbeke et al. [27] with a test chamber built inside the facility. However, this chamber was removed for the experiments described in this paper. The test facility has internal dimensions of 12.0 × 5.3 × 4.9 m (length x width x ridge height) yielding a volume of 251 m³. Both concrete sidewalls have ventilation openings of 0.5 × 4.5 m with a depth of 0.2 m. The width of these vents can be changed by placing wooden boards that cover parts of the opening area. The ridge of 0.3 × 4.0 m has upright flanges of 0.3 m and can be sealed completely (see Fig. 2). During the monitoring period, no large obstructions were present in the area surrounding the test facility, within a radius of 40 m. Following the rule of good practice, the side vents are oriented SW [32], which is the prevailing wind direction in Flanders. To visualize leakages, all vents were closed and a fan was installed at vent A to induce an internal pressure of 100Pa. All major leaks were visualized with smoke tests and sealed where possible until no more smoke was observed to escape from the building. Furthermore, Etheridge [33] states that with the larger openings adventitious leakage can be neglected.

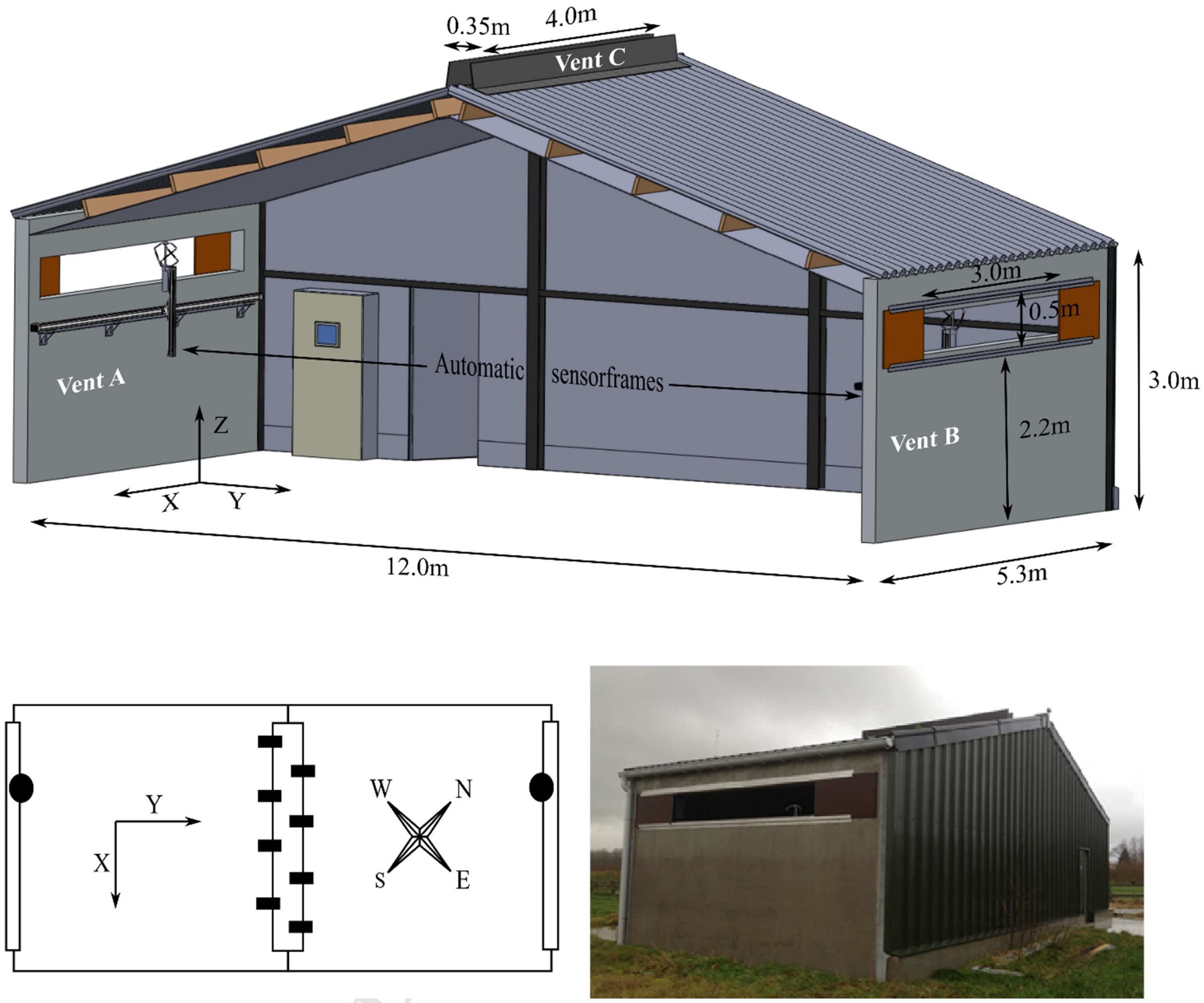

Fig. 1: 3D drawing and picture of the test facility built at the Institute for Agricultural and Fisheries Research. Sketch: Top view of the test facility with the X-Y coordinate system of the anemometers compared to the wind rose. ●: moving 3D ultrasonic anemometer in side vent; ■: static 2D ultrasonic anemometer in ridge.

2.2 Hardware configurations

An automatic sensor frame developed and described in detail by Van Overbeke et al. [28] was used. This frame was used to perform an automated traverse movement by a 3D ultrasonic anemometer or 3DS (Thies® 4.3830.22.300, Göttingen, Germany) across the in- or outlet area of a vent. The sensor frame consisted of a connected horizontal (4.5 m) and vertical (0.7 m) linear guiding system. On top of the vertical guiding system a 3DS was installed. The movement of the guiding systems and therefore the sensor itself were driven by two PLC controlled servomotors. Air velocity data logged whilst the sensor movement was carried out were not accounted for in further calculations. Two of these frames were positioned on the inner walls of the test facility beneath Vents A and B (Fig. 1).

In the experimental set-ups where the ridge was kept open (see 2.4), 8 2D ultrasonic anemometers or 2DS (Thies® 4.3820.02.300, Göttingen, Germany) were fixed inside the ridge. The positioning of these sensors can be seen in Fig. 2. Holes were cut in the purlins in order to house the sensors. However, due to a lack of depth, the sensor heads were not located in the centre of the ridge but 2 cm further away. This was the only feasible sensor set-up without causing larger flow disturbances in the ridge. A calibration conducted by Deutsche WindGuard Wind Tunnel Services GmbH showed a standard uncertainty of max. 0.05 m/s in a range of 0.557–5.470 m/s for both the 2DS and 3DS.

In order to acquire more detailed information on the cross-sectioned air velocity profile through the ridge, 1D hotwire anemometers were used. A total of 9 hotwire anemometers were fixed across the width of the ridge (Fig. 2:B) (in the centre: TSI®, Air Velocity Transducer Model 8455, USA, Shoreview, and remaining hotwires: E+E Elektronic®, EE66-VC5K1000, Germany, Engerwitsdorf). According to the manual the 8455 hotwire has an accuracy of ± 2.0% of the reading or ± 0.5% of full scale of selected range. The selected range was 0.0 - 5.0 m/s. The EE66 model has an accuracy of ± 0.06m/s + 2 % of the measured value. All hotwire anemometers were recently calibrated.

A meteorological tower (meteomast) equipped with one 2DS at a height of 10 m was installed South-East of the test facility. All sensors were connected to a datalogger (dataTaker® DT85M, Australia) through a serial interface (RS422). This allowed for a simultaneous readout of all sensors. The data was collected at 50 Hz and 33 Hz for the 2DS and 3DS, respectively, and stored as 1s averages. Hotwire anemometers were logged at 1 Hz.

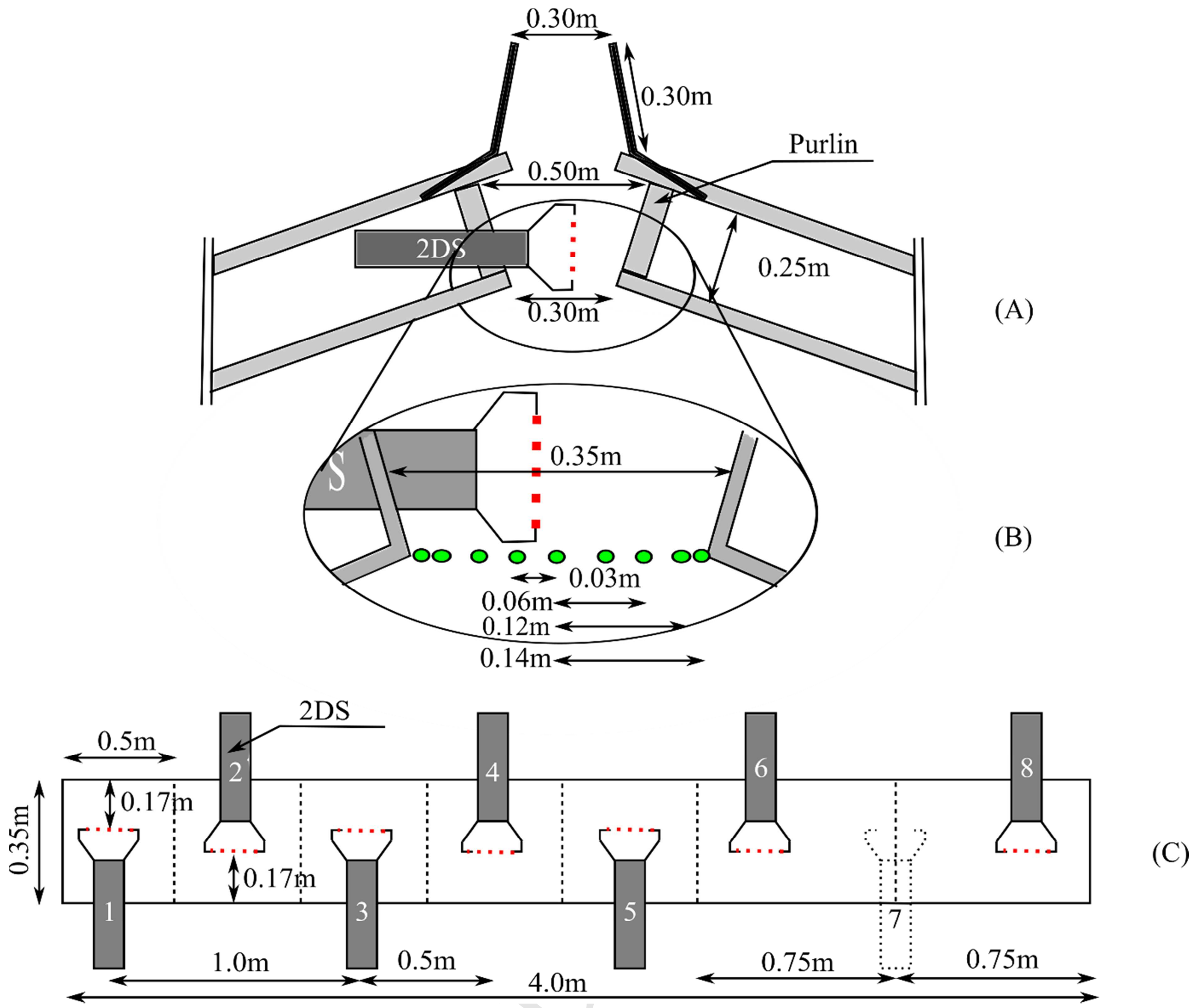

Fig. 2: A: Cross section of the ridge with an installed 2D ultrasonic anemometer. B: Green circles represent measurement locations of the 1D hotwire anemometers (not to scale). They are located beneath 2D sensor 6. One of the hotwires malfunctioned and is marked with an ×. C: Top view of the ridge with 8 2D ultrasonic anemometers and their allocated outflow areas. Dotted red lines represent the measuring path of the 2D ultrasonic anemometer. 2D sensor 7 malfunctioned and was removed.

2.3 Ventilation rate measurement method

2.3.1 **Data collection at side and ridge vents**

Gathering the air velocity data at side vents was performed by the method developed by Van Overbeke et al. [27]. The method consisted of dividing the volume immediately downstream of the vent opening into cuboids with the size of the measuring head of the 3DS (0.25 × 0.25 × 0.125 m, L × B × H), further referred to as measuring volumes. Each volume was sampled consecutively for 10 s by a 3DS. The time it took to move the sensor to the next volume and start measuring was 2 s on average. Fig. 3

illustrates how this method was applied to an opening of size 0.5 × 3.0 m. To capture the time dependent velocity profile, the complete vent was consecutively traversed 10 times. Hence each measuring volume was sampled for a total of 100 s. Each measuring cycle was repeated cyclically. For more details the reader is referred to Van Overbeke et al. [27].

For the ridge (Vent C) all measuring points were monitored simultaneously. Air velocity data at the ridge was collected over the same time period in which the side vents were traversed 10 times. 2D sensor number 7 was removed from the ridge due to software errors and could not be replaced during further experiments. The in- or outlet areas related to sensors 6 and 8 were widened to fill this gap (see Fig. 2C). The width of the ridge was taken at the centre of the 2DS measuring path. Therefore the elementary surface area per 2DS was considered to be 0.35 × 0.50 m for sensors 1 to 5 and 0.35 × 0.75 m for sensors 6 and 8. Only the velocity component normal to these areas was utilized in the calculations.

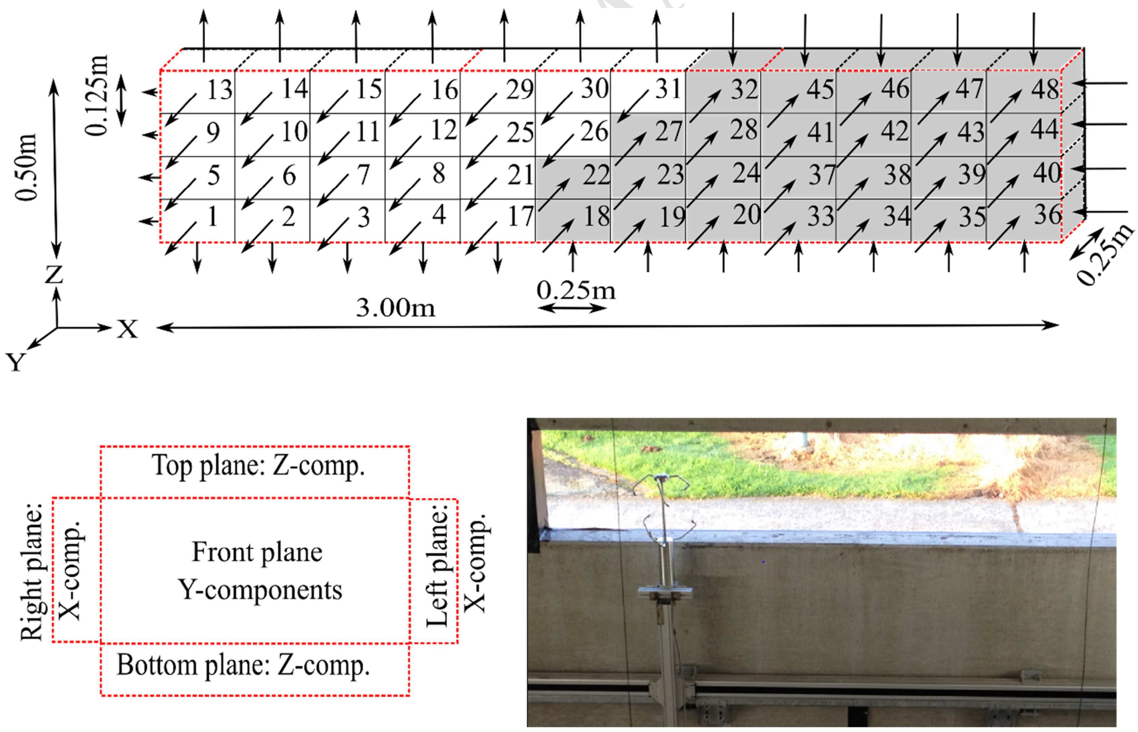

Fig. 3: Top sketch: Impression of a velocity profile measured in Side Vent B with North-Western winds (not an actual measurement). In which the vent is divided into 48 measuring volumes or 88 elementary surfaces, arrows represent the velocity components sampled at each surface. Grey and white areas represents air flowing out of and into the building, respectively. Airflow through grey surfaces is added to the total outflow rate (Q_{out}) airflow through white surfaces to the total inflow rate (Q_{in}). Bottom sketch: Names of the different planes and

the velocity components related to these planes. Picture partly shows the 3D ultrasonic sensor on the automatic sensorframe in the 3m wide vent.

2.3.2 *Determination of the ridge pipe factor*

An additional consideration had to be made in view of the calculation of the in- and outflow rates through the ridge. As can be seen from Fig. 3 and Fig. 2C the area related to a velocity measurement in the ridge is almost 6 times larger than that in the side vents. Therefore a different data processing method was needed for the ridge.

When the velocity profile in a vent is known, the average velocity (V_{avg}) can be found and multiplied by its related outlet area to obtain the airflow rate. However, only the velocity in the longitudinal central axis (V_c) of the ridge was measured in this set-up. Assuming V_c to be representative of the total outflow area can lead to large inaccuracies of the airflow rate [6]. The ratio between V_{avg} and V_c is represented by the pipe factor ($PF = V_{avg}/ V_c$). For instance, the PF for a laminar flow through a wide rectangular channel is 2/3 [34]. However for a turbulent flow, which is more likely in the ridge, determination of the PF is more complex and is dependent on the Reynolds number and roughness coefficient of the duct. A PF of 0.91 is given for a Reynolds number of 10^6. Although the ridge is not a truly “smooth rectangular duct”, the expected value of the PF is situated between 0.66 and 0.91 [34]. Hotwire anemometer measurements in the ridge were carried out to give an estimate of the general shape of the velocity profile. The measurements were taken directly beneath sensor 6 (see Fig. 2B). Sensors were positioned at the centre and at 0.03, 0.06, 0.12 and 0.14 m to the left and right of the centre. The hotwire located at 0,03 cm to the left of the sensor malfunctioned and no valid data could be retrieved. All hotwires measured simultaneously at a frequency of 1Hz and results were based on 5 minutes averages. From these point measurements, a velocity profile was composed from which the V_{avg} was calculated. In this velocity profile, the velocity at the borders was considered zero. V_c was measured by the hotwire in the centre. A PF was calculated for each 5 minute measurement interval.

2.3.3 **Calculation of the ventilation rate**

The method for calculating the ventilation rate used in Van Overbeke et al. [27] delivered satisfactory results for a small cross ventilated chamber with vents of 0.5 × 1.0 m. The agreement between the airflow rates measured in both vents was in the range of (-1 ± 11)%. However, when in a vent the average air velocity was lower than 0.05m/s or winds were parallel to the vents, the relative measurement error increased.

With a wind incidence angle parallel to the vents, the vents acted partly as an inlet and partly as an outlet [35]. Therefore, when the average airflow over the total vent area was taken, a result was found close to zero, which yielded large relative errors. To account for these situations, the in- and outflow rates through a vent should not be averaged, and for this reason, the data analysis procedure had to be slightly modified.

Fig. 3 clarifies that the velocity components that are accounted for depend on the location of the measuring volume. In each volume the air velocity components were allocated to their related elementary surfaces. Each elementary surface was characterized by a set of 100 air velocity data points obtained through the data gathering method described in 2.3.1. Such a set was subdivided into positive and negative air velocities. A time weighted average was taken of the positive and negative subsets separately and multiplied by the related elementary surface areas to obtain the airflow rate flowing in and out of the building through that area, respectively. The same procedure was followed in the ridge vent but all measured air velocities were multiplied by the PF (see 2.3.2). As a final step, all elementary in- and outflow rates of all vents were summed into a total building inflow (Q_{in}) and outflow rate (Q_{out}), respectively (Formula 1)

$$Q_{in} = \sum_{j=1}^{m} \sum_{i=1}^{n} (v_{i+} \cdot A_i \cdot 3600)_j \qquad [1]$$

Where:

Q_{in}: the total building inflow rate (m^3/h); m: the number of vents (2 or 3 depending on whether or not the ridge is open); n: number of elementary surfaces in the vent (varying between 7 and 88 depending on the related vent and set-up); v_{i+}: the time weighted average of the velocity component contributing to the inflow rate through elementary surface “i” (m/s); A_i: the area of the elementary surface “i” for which the velocity component was measured (m^2).

Formula 1 was used to calculate the total building outflow (Q_{out}, m^3/h) by substituting v_{i+} to v_{i-}, which is the time weighted average velocity component contributing to the outflow rate through an elementary surface "i".

According to the law of mass conservation, applied to an incompressible medium, the inflow rate should equal the outflow rate. Therefore the relative measuring error (E_q) between Q_{in} and Q_{out} (Formula 2) was used as a measure for the accuracy of the method. Throughout the experiments the average value between Q_{in} and Q_{out} was taken as the reference ($Q_{avg} = (Q_{in} + Q_{out})/2$). The method was considered to be sufficiently accurate when the E_q remained under 20% under a large variety of external wind conditions. This was based on studies, also using ultrasonic anemometer measurements to measure the airflow rate, where the relative measurement errors between the in- and outfluxes ranged from -34% to 37% [36–39].

$$E_q = \frac{Q_{in} - Q_{out}}{Q_{avg}} 100 \qquad [2]$$

2.4 Imposed measurement conditions

In Van Overbeke et al. [27] a ventilation rate measuring method was validated for naturally ventilated openings of 0.5 × 1.0 m in a cross ventilated room. In this current study, the final goal was to determine the airflow rates through the test facility featuring an open ridge and side vents of 0.5 × 3.0m, rendering the test facility more representative for conditions in commercial animal houses. Therefore, three different set-ups of the test facility were examined.

In set-up 1 the opening areas of Vents A and B were 0.5 × 3.0 m and 0.5 × 1.0 m, respectively, and the ridge was closed. Here Vent B was taken as the reference against Vent A, which allowed the validation of the measuring method applied to a wider vent (see 3.2.1). Vent B was bordered with a flange measuring 1.14 × 0.64 × 0.30 m, to simulate the conditions of the measurements made by Van Overbeke et al. [27]. This flange was built to allow for a more unidirectional flow pattern. No flange was present around Vent A. Van Overbeke et al. [27] concluded that measuring the X- and Z-components at the borders of the 0.5 × 1.0 m vent was necessary to obtain the most accurate measuring method. In set-up 1 this was re-evaluated with a 0.5 × 3.0 m vent.

In set-up 2 the opening areas of Vents A and B were 0.5 × 3.0 m and the ridge was kept open. This allowed the validation of the measurement method in the ridge (see 3.2.2). No flange was present around Vents A or B.

In set-up 3 the ridge was open along with vents A and B. However, the width of Vent B was set to 1.0 m in order to force more air towards the ridge in conditions when Vent A was the inlet. This increased the ridge's relative contribution to the outflow rate. Vent B was again bordered with the flange. Set-up 3 was built to test the effect on the E_q of a predominantly ridge ventilated set-up as compared to set-up 2. This allowed for an additional check of the ridge measurement method.

2.5 Experimental conditions

In Fig. 4 an overview is given of the wind conditions for set-ups 1, 2 and 3. The distribution of the wind incidence angles are given in the polar plots together with the relative and cumulative wind speed frequencies. These parameters were measured at the meteomast and were based on the averages taken from a total of 443, 833 and 710 airflow rate measurements in set-up 1, 2 and 3, respectively. Because of the building orientation, the angle of 180° corresponds to the south-west direction. This allowed a clearer representation of the wind incidence influences. In set-up 1, all directions except for south-east incidence angles were covered (Fig. 4 A). While, in set-ups 2 and 3, only a relatively limited amount of data is coming from wind directions other than south to southwest. All measurements were made between December 2014 and March 2015. The proposed measuring method does not differentiate between the source of the airflow, i.e. originating from the stack or wind effect. There were no heat sources in the test facility and the relatively large vents were permanently opened to allow continuous renewal of the internal air volume. Therefore, the difference in temperature between the in- and outdoor climate was assumed to be minimal. Hence, the influence of the stack effect on the distribution of the flows through side- or ridge vents was not examined and all airflows were attributed to the wind effect.

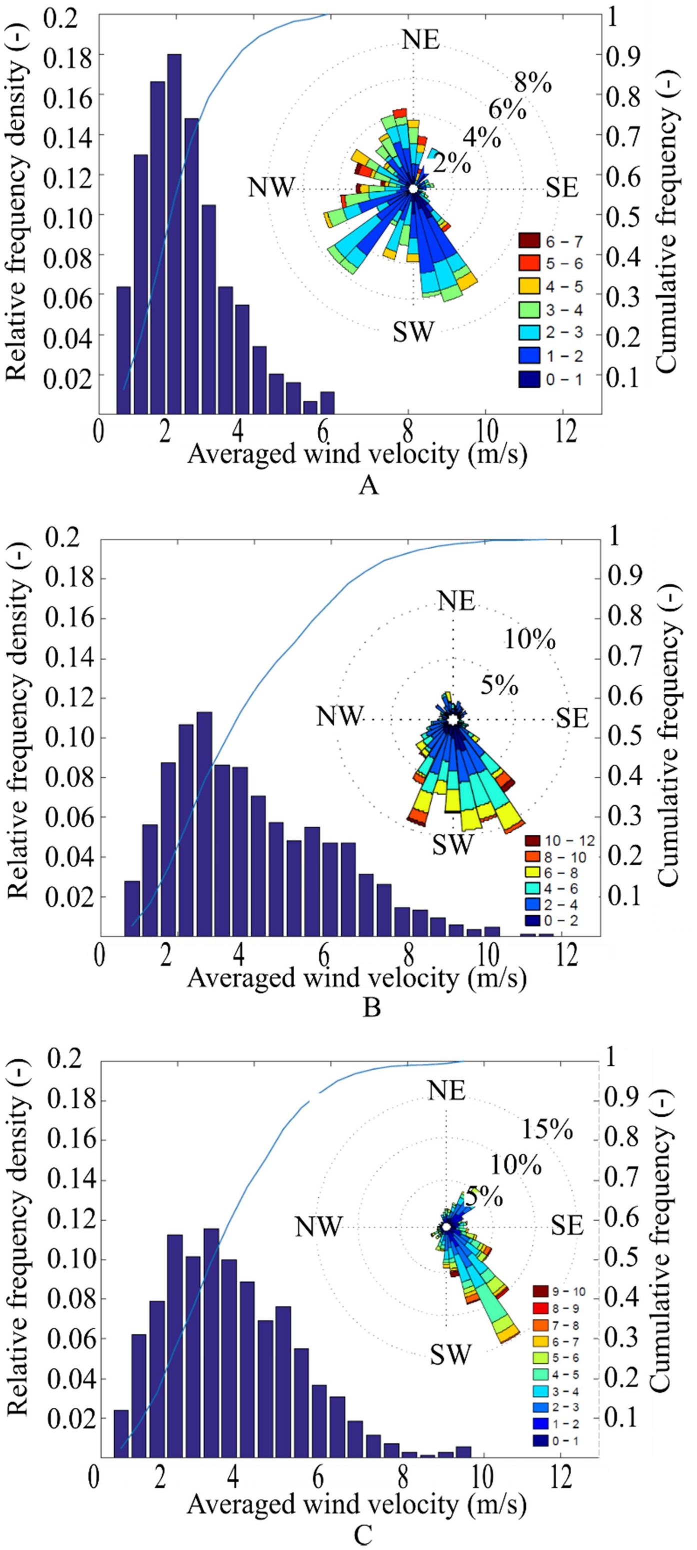

Fig. 4: A, B and C: Relative and cumulative wind frequencies and polar plot of the wind direction measured at the meteomast during measurement periods with (A) set-up 1 from 04/2014 to 08/2014, (B) set-up 2 from 12/2014 to 03/2015 and (C) set-up 3 from 08/2014 to 12/2014.

3 Results and Discussion

3.1 Evaluation and validation of the measurement method

3.1.1 Conditions of cross ventilation with closed ridge (set-up 1)

<u>*Relative measurement error*</u>

In Fig. 5:A the relative measurement error of the ventilation rate (E_q) as a function of wind incidence angle is shown. The E_q remained between (5 ± 8)% and in none of the wind incidence ranges the established tolerance level of ± 20% was surpassed.

Therefore, it can be seen that the method developed by Van Overbeke et al. [27] was successfully adapted and transferred to the larger vent of 0.5 × 3.0 m.

In Table 1 the relative contributions of Vents A and B to the total in- or outflow rates, classified amongst 4 ranges of wind incidence angles are shown. In the wind direction ranges of 135° to 225° and 315° to 45° a relatively stable distribution is found. Higher percentages suggest fixed in- and outlets in these situations. However, the distribution changes entirely in the ranges of 45° to 135° and 225° to 315°. These ranges contain wind directions parallel to the vents. The relative contribution to the inflow rate ranging from 34 to 69% for both Vents A and B indicates that these vents acted simultaneously as both in- and outlets. Nevertheless, even in these complex situations E_q remained between ± 20% (Fig. 5:A), it can be stated that the measurement method and data analysis were robust. In Fig. 6:A the change in relative in- or outflow contribution as a function of the wind incidence angle can be seen. From approximately 50° onward, the relative contributions begin to shift drastically to become stable again at around 120°. The amount of data from these wind directions was too low to see a clear start and end of this unstable region. However, the same trend is much clearer in the range of 225° to 315°, due to the larger amount of measuring points. There, the range in which the side vents shift from inlet to outlet and vice versa is approximately 250° to 300°.

Table 1: Relative contribution (%) of Vents A and B to the total in- or outflow rate through the test facility for set up 1, classified into 4 different ranges of wind incidence angles.

	0 - 45° and 315 - 360°	45 - 135°	135 - 225°	225 - 315°
Vent A_{in} (%)	11 ± 15	58 ± 32	96 ± 7	69 ± 34
Vent B_{in} (%)	92 ± 16	41 ± 34	5 ± 5	34 ± 33
Vent A_{out} (%)	-82 ± 8	-53 ± 23	-19 ± 11	-44 ± 26
Vent B_{out} (%)	-15 ± 9	-48 ± 25	-79 ± 9	-53 ± 24
n	111	28	173	131

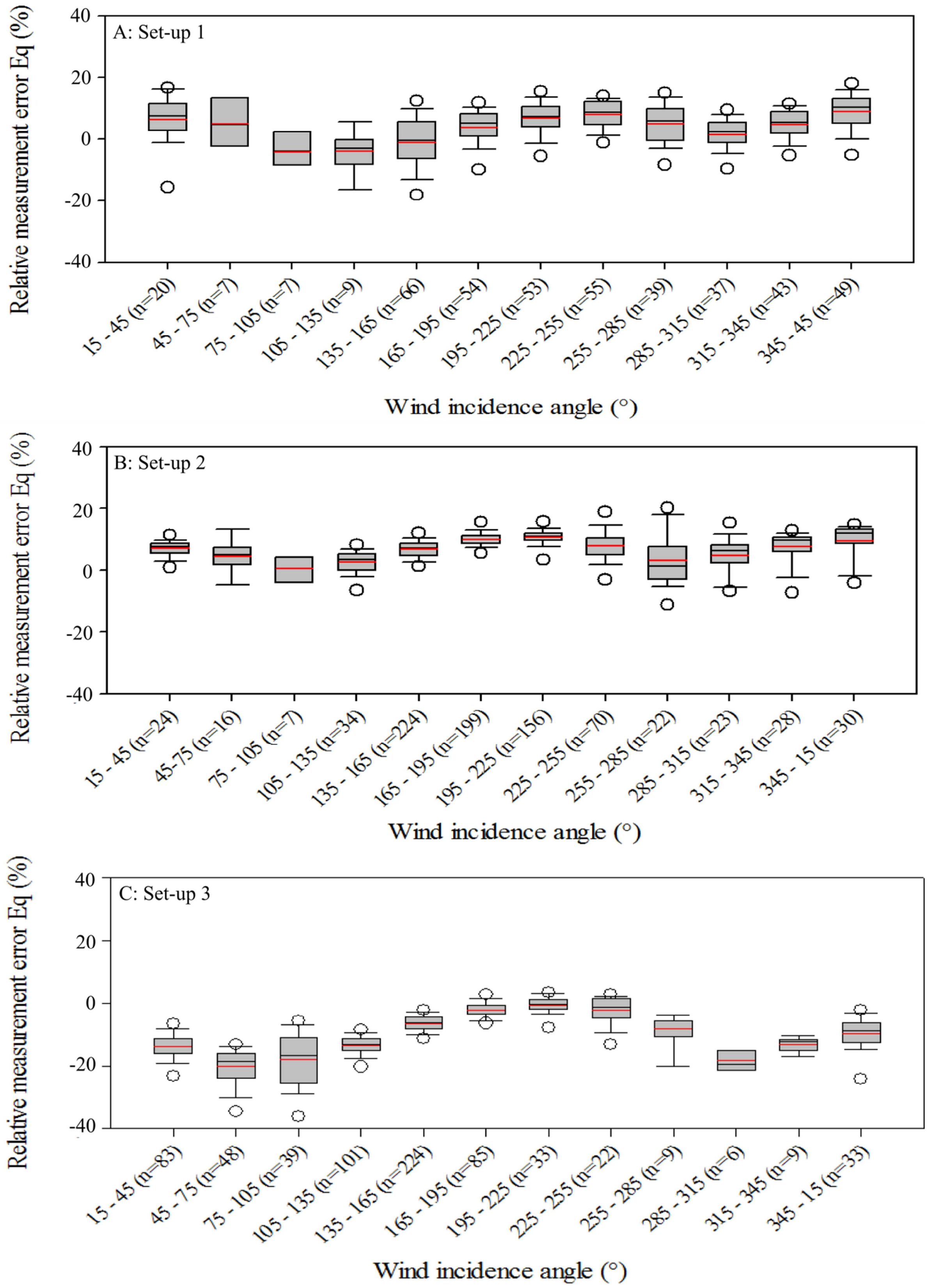

Fig. 5: Boxplots of relative measurement error as a function of wind incidence angle for set-ups 1 (A), 2 (B) and 3 (C). The red lines in the boxes are averages, the black medians.

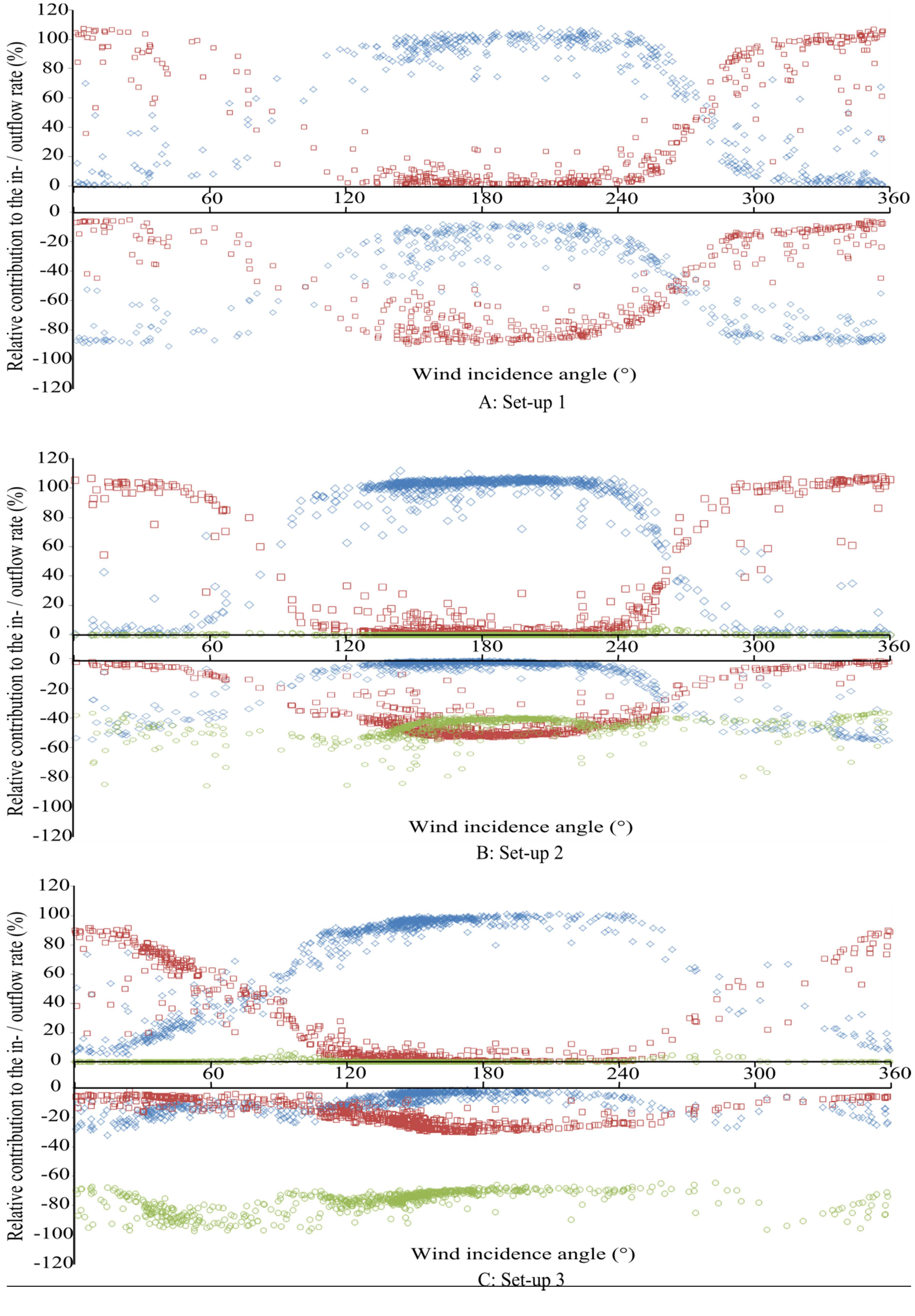

Fig. 6: Relative contributions of Vent A, B and C to the in- or outflow rate for set-ups 1 (A), 2 (B) and 3 (C), with ◇: flow through Vent A (blue); □: flow through Vent B (red); ○: flow through Vent C (green); positive and negative values are relative inflow and outflow

contributions, respectively.

Need of 3D measurements

In Fig. 7: E_q values as a function of the wind incidence angle are shown, averaged over wind direction intervals of 30°. The in- and outflow rates measured in Vent A that are added to Q_{in} and Q_{out}, respectively, are calculated in 4 different ways. Namely, by accounting for different velocity components: (a) only the Y-components; (b) the Y- and X-components; (c) the Y- and Z-components and finally (d) all three components. Fig. 3 clarifies where these components were measured. The opening areas related to the Y- and Z- components (Y: front plane, Z: top and bottom plane) were considerably larger than that of the X-components (left and right plane). The in- and outflow rates in Vent B were calculated accounting for all components, as was recommended for this type of vent in Van Overbeke et al. [27]. In Fig. 7 it can be seen that only accounting for the Y-components in Vent A resulted in larger relative measurement errors, in the range of (11 ± 35)%. Highest errors were found in cases where the wind was blowing perpendicular to the vents. Adding the Z-components to the calculation lowered the range of E_q to (5 ± 8)%. As seen in Fig. 7, this result is approximately equal to the result obtained by including all components. Therefore, including the Z-components was an essential part of the measuring method for this set-up. The X-component on the other hand, did not add a considerable improvement to the relative measurement error and, in the conditions of this study, could be omitted. However, for future study of flow patterns around the vents, all components deliver valuable information. Therefore, none of the components are omitted in further measurements throughout this paper.

It must be noted that the large influence of the Z-components is partly attributable to the top and bottom plane being of almost equal area as the front plane (see Fig.3). The larger the vent, the higher the influence of the front plane will be compared to that of the top and bottom plane. Therefore in very large vents, such as those found in cattle houses, measuring only the Y-component could be sufficient.

This outcome seems to be in agreement with other studies where the ventilation rate in NV buildings is determined via anemometer measurement data multiplied by vent area. Also there, only the velocity component normal to the vent opening is usually considered [38–40]. However, compared to the present study, the applied vent areas related to the sampling points are much larger in these studies e.g. from 0.9 m² [36] and 2.1 m² [38] up to 110 m² [39]. Also measurements close to the vent's borders are mostly avoided in these studies. Air velocities are generally highest in the centre of the openings [41] as there is little influence of the vent's borders. Therefore these velocities can overestimate the in- and outflow rates when multiplied by the vent area. It is in such cases that applying mass conservation as a validation tool can be misleading as this overestimation cannot be identified. This might explain why, even when applying a relatively lower measurement density, the in- and outflow rates can still agree fairly well, e.g. 12 to 19% [39], 1 to 28% [37], -3 to 37% [38] and -34% to 8% [36] (percentages are calculated similar to equation [2]). Therefore, when the measurement set-up does not sufficiently account for the spatial variability of the velocity profile, errors can occur which could remain undetected when validating with the mass conservation principle.

Although the present study also relies on this principle, the reliability of our results was increased by the high measurement density and the large range of measurement conditions under which the method was validated.

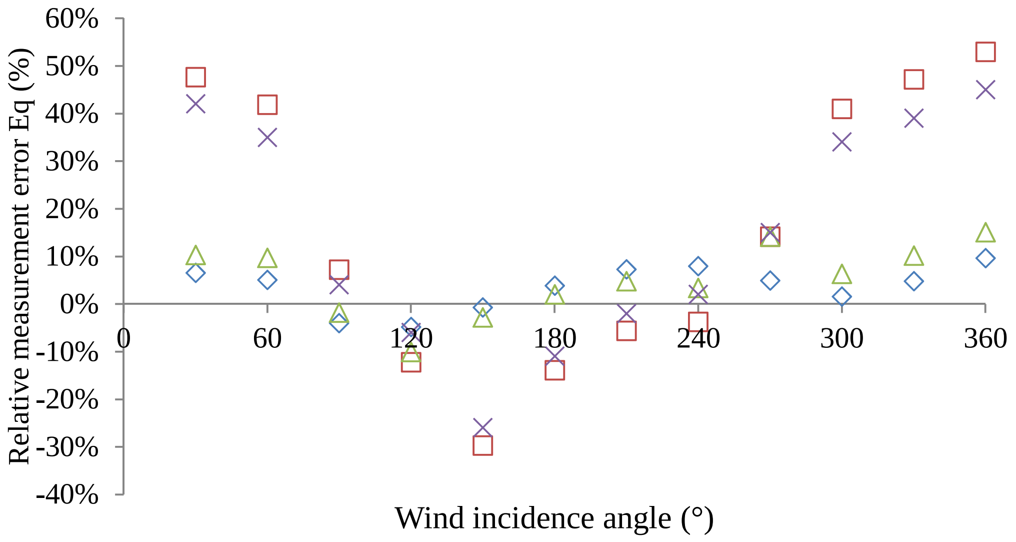

Fig. 7: The relative measurement error (E_q, %) as a function of wind incidence angle. The in- and outflow rates through Vent A are calculated with four different methods: □: only accounting for the Y- velocity component (red); △: accounting for the Y- and Z- velocity

components (green); ×: accounting for the Y- and X- velocity components (purple); ◇: accounting for all velocity components (blue). The in- and outflow rates through Vent B (needed for the calculation of E_q) were calculated accounting for all components. For each method the relative measurement errors (%) were calculated and averaged within intervals of wind incidence angles of 30°.

3.1.2 **Conditions of cross and ridge ventilation (Set-up 2)**

Pipe factor

In order to establish a PF value of the ridge, a total of 186 velocity profiles were determined with measurements carried out over a period of 4 days. In Table 2 the velocity profiles were subdivided into 8 centre speed ranges, i.e. the wind velocity measured by the hotwire anemometer at the centre of the velocity profile in the ridge (Fig. 2:B). In Table 2 it can be seen that an increasing centre speed resulted in a slight decrease in PF. Linear regression analysis indicated a rather weak, but present, correlation between the centre speed and the associated PF's (R^2=0.42, $P<0.001$). In Fig. 8, where 7 of these velocity profiles are shown, it can be seen that higher centre speeds resulted in profiles with a more “bullet shaped” profile. Such profiles suggest laminar flows, which are characterised by lower PF values [34]. The lower centre speeds had a more homogenous distribution of the air velocity, and suggest turbulent profiles with a higher PF value. Although the profiles were not symmetrical, the centre speed mostly remained the highest value.

The wind incidence angle during the tests varied between 105° and 168° (N= 152) and between 284° and 314° (N=22), however only the 105 – 168° range was considered. Linear regression analysis showed a relatively weak correlation between wind incidence angle and the associated PF's (R^2=0.27, $P<0.001$). Nevertheless, one may notice that larger variations in wind incidence angles might have a significant effect on the shape of the velocity profile.

The ridge experiments indicated that the PF might be dependent on wind incidence angle and air velocity in the ridge. However within the ranges of our measurements the correlations were weak. Hence, under the conditions met here, the PF was considered to be constant. Based on the average taken of all velocity profile measurements, a PF of 0.78 was withheld to calculate the airflow rates in set-ups 2 and 3.

Table 2: Pipe factors (PF, dimensionless) related to wind speeds at the centre of the velocity profile measured in the ridge.

Centre speed range (m/s)	PF ± SD*	n
0.50 to 0.74	0.79 ± 0.03	11
0.75 to 0.99	0.81 ± 0.04	46
1.00 to 1.24	0.79 ± 0.02	13
1.25 to 1.49	0.79 ± 0.02	14
1.50 to 1.74	0.77 ± 0.02	31
1.75 to 1.99	0.76 ± 0.02	21
2.00 to 2.24	0.75 ± 0.02	34
2.25 to 2.65	0.75 ± 0.02	16

*SD: standard deviation of the mean

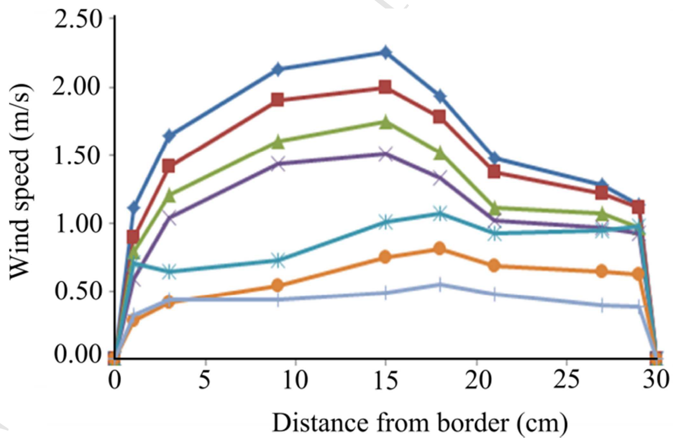

Fig. 8: Velocity profiles with different centre speeds measured in the ridge with +: 0.50 m/s (light blue); ●: 0.75 m/s (orange); ∗: 1.00 m/s (blue); ×: 1.50 m/s (purple); ▲:1.75 m/s (green); ■:2.00 m/s (red); ♦:2.25 m/s (dark blue). The velocities at the borders, i.e. at 0 and 30cm were assumed zero and do not represent measured values.

Relative measurement error

Values of E_q varied in the range of (8 ± 5)% for the measurements in set-up 2, successfully remaining below the ± 20% limit for each separate wind incidence angle range (Fig. 5:B). As this is in agreement to what was found in Set-up 1, the measurement method applied to the ridge was considered to be effective.

Although in this set-up E_q seems to reach lower values at wind incidence angles parallel to the vents, it presented an increased variability, as compared to set-up 1.

In Fig. 6:B the relative contributions to the total inflow and outflow are shown. For all wind directions the contribution of the ridge to the inflow was nearly non-existent (0 ± 1) %. This means that the ridge can be considered a full and permanent outlet, independent of the wind incidence angle. A wind tunnel study by [42]) showed that at wind incidence angles close to 270° or 90° part of the ridge opening function fluctuated between in- and outlet. In present study it was assumed that the short length of the test facility's ridge compared to those found in commercial animal houses diminished this effect. The contribution of the ridge to the total outflow rate was relatively constant and therefore also independent of the wind incidence angle. The outflow contribution of the ridge varied in the range of (46 ± 7)%. Vents A and B showed a similar behaviour as in set-up 1 where the in- or outlet character of the vents were determined by the wind incidence angle. Again the wind incidence ranges in which the inlets completely changed into outlets and vice versa are 50° to 120° and 250° to 300°. At approximately 90° and 270° there were cases in which both Vents A and B accounted for 50% of the inflow rate. The closer the wind incidence angle was to 180° or 360°, the higher the contribution to the inflow of Vent A or B, respectively. Fig. 6:B is summarised in 4 ranges of 90°.

Table 3 where the data is classified amongst 4 ranges of 90°.

Table 3: Relative contribution (%) of Vents A, B and C to the total in- or outflow rate through the test facility for set up 2, classified into 4 different ranges of wind incidence angles

	0 - 45° and 315 - 360°	45 - 135°	135 - 225°	225 - 315°
Vent A_{in} (%)	3 ± 7	69 ± 37	103 ± 5	70 ± 37
Vent B_{in} (%)	101 ± 9	32 ± 37	2 ± 4	32 ± 36
Vent C_{in} (%)	0 ± 0	0 ± 0	0 ± 0	1 ± 1
Vent A_{out} (%)	-46 ± 8	-15 ±13	-3 ± 2	-18 ± 15
Vent B_{out} (%)	-4 ± 2	-28 ± 13	-48 ± 6	-33 ± 14

Vent C_{out} (%)	-46 ± 9	-55 ± 8	-44 ± 6	-46 ± 6
n	82	57	579	115

3.1.3 Conditions of cross and adapted ridge ventilation (Set-up 3)

In Table 4 and Fig. 6: C it can be seen that the relative outflow rate contribution of the ridge was 20 to 30% higher than in set-up 2. This effectively increased the contribution of the measurement method of the ridge on the relative measurement error. Values for E_q of (-9 ± 7)% were found for the measurements in set-up 3, again remaining under the 20% limit for all wind incidence range (Fig. 5: C). However, compared to Set-ups 1 and 2, a shift towards more negative values of Eq can be seen. In the ranges 45°-75°, 75°-105° and 275°-315° the values of Eq average around -20%. Although it is to be expected that in these ranges the measurement errors increase due to the more complex airflow patterns, it is not clear why this particular set-up seems to increase this effect. To determine whether the asymmetry of the side vent sizes was one of the influencing parameters, a more detailed view on velocity profiles and related indoor airflow patterns is necessary. It cannot be determined whether these negative values were due to an under- or overestimation of the inflow or outflow rate, respectively.

It should be noticed that the increase in the ridge's relative outflow contribution was only expected in situations where Vents A and B were full inlet and outlet, respectively. In such cases the outlet area through Vent B was smaller than that of the ridge by a 3-fold. However, the increase in relative outflow contribution seemed to be approximatelly constant over all wind directions, and was in the range of (77 ± 7)%. Combined with the results found for set-up 2, it can be infered that the relative outlet contribution of the ridge is independent from the wind incidence angle, but strongly dependent on the side vents configuration. Experiments with more varied vent configurations should allow to derive the relation between the ridge's relative outlet contribution and the vent configuration.

In the range of 315 – 45°, it was expected that Vent A would be completely an outlet with a relative inflow contribution of nearly 0%. However an inflow contribution of (20 ± 14)% was found (see Table 4). This effect can also be seen in Fig. 6:C. There, the ranges in which Vents A and B changed from approximatly 0 to 100% outlet contribution widened considerably towards 360° as compared to Fig. 6:A and B. This means that even with wind incidence angles near to 360°, there existed cases where Vents A and B were still partially in- and outlet. These situations are more challenging for the measurement method and could be a partial explanation for the lower calculated $E_{q.}$ This also suggests that the wind incidence angles in which a side vent can be considered a full in- or outlet is dependent on vent size configuration. Therefore, studies that rely on the assumption that a vent is a permanent outlet, e.g. for emission rate measurements, should account for this effect. In such cases, special care should be taken when the vent has a variable area, as when curtains are used.

Table 4: Relative contribution (%) of Vents A, B and C to the total in- or outflow rate through the test facility for set up 2, classified into 4 different ranges of wind incidence angles

	0 - 45° and 315 - 360°	45 - 135°	135 - 225°	225 - 315°
Vent A_{in} (%)	20 ± 14	66 ± 24	96 ± 3	81 ± 21
Vent B_{in} (%)	74 ± 15	25 ± 23	2 ± 2	14 ± 17
Vent C_{in} (%)	0 ± 0	1 ± 1	0 ± 0	1 ± 2
Vent A_{out} (%)	-17 ± 6	-13 ± 4	-5 ± 3	-12 ± 6
Vent B_{out} (%)	-7 ± 3	-14 ± 5	-25 ± 4	-20 ± 5
Vent C_{out} (%)	-82 ± 7	-82 ± 7	-73 ± 4	-72 ± 6
n	125	188	360	37

4 Conclusions

A naturally ventilated test facility was adapted for cross and ridge ventilation schemes, to which an automated airflow rate measuring technique was applied. For the side vents, a technique developed by Van Overbeke et al. [27] was successfully adapted to larger vents (0.5 × 3.0 m) and a new airflow rate measurement set-up for the ridge was validated. A pipe factor of 0.78 was determined and attributed to the ridge. Detailed measurements of the velocity profiles in the vents were possible and the in- and outflow rates in each vent were processed separately.

It was found that the method for the side vents should account for all air velocity components, while the vertical component at the top and bottom vent borders and the component normal to the vent opening were essential to the calculations.

When side and ridge vents were fully opened, a relative measurement error between the building's total in- and outflow rate of (8 ± 5)% was found, successfully remaining below the self-imposed limit of 20%.

The relative contribution of a side vent to the building's total in- or outflow rate was dependent on the wind incidence angle. The range of wind incidence angles in which side vents were completely in- or outlet depended on the size of the vents. Outside these ranges, the vents gradually changed from outlet into inlet or vice versa, as a function of wind incidence angle.

The ridge had no considerable contribution to the inflow rate and was considered as a full and permanent outlet, independent of wind direction. Moreover, the relative contribution of the ridge to the total outflow rate was relatively constant since a standard deviation of only 7% was found throughout all measured wind incidence angles. However, measurements in 2 different set-ups showed that the ridge's relative outflow contribution was dependent on the side vents configuration.

Due to the complexity of the measuring technique it is practically and economically unfeasible to transfer the technique to a full size animal house. However, as the developed test facility is equipped with a validated measuring technique, it can be used for comparison with new and existing airflow rate measuring techniques for the use in naturally ventilated buildings. The design of these new techniques should be focussed on the possible transfer to very large vent sizes such as those found in cattle houses. Modelling is a possible way to reduce the complexity of the measuring technique. The test facility can be used to develop, validate and test such models. Although these models will probably not be directly transferable to other buildings, proving that certain modelling approaches work in the test facility can provide useful information to guide the research on full scale animal houses.

Acknowledgements

This study was conducted during the Agricultural Research Project IWT090946, which was funded by the Agency for Innovation by Science and Technology (IWT) of the Flemish government. The authors also thank the technicians at ILVO for their advice and support.

References

[1] EEA, Air pollution fact sheet 2014 - European Union (EU-28), (2014).

[2] NEC-Directive, Directive 2001/81/EC of the European parliament and of the council, 2001.

[3] Kyoto-Protocol, Kyoto Protocol to the United Nations Framework Convention on Climate Change, United Nations, 1998.

[4] K. Wark, C.F. Warner, W.T. Davis, Air Pollution: Its Origin and Control, 3rd ed., Prentice-Hall, 1998.

[5] S.J. Hoff, L.D. Jacobson, A.J. Heber, J. Ni, Y. Zhang, J.A. Koziel, et al., Real-Time Airflow Rate Measurements from Mechanically Ventilated Animal Buildings, J. Air Waste Manage. Assoc. 59 (2009) 683–694. doi:10.3155/1047-3289.59.6.683.

[6] S.E. Ozcan, Techniques to determine ventilation rate and airflow characterstics through naturally ventilated buildings, Doctoral dissertation, K. U. Leuven, K.U.Leuven, 2011. doi:ISBN 978-90-8826-205-0.

[7] L.D. Albright, Environmental Control for Animals and Plants. St. Joseph, MI: ASAE., 1990.

[8] Y. Li, A. Delsante, Natural ventilation induced by combined wind and thermal forces, Build. Environ. 36 (2001) 59–71. doi:10.1016/S0360-1323(99)00070-0.

[9] M. De Paepe, J.G. Pieters, W.M. Cornelis, D. Gabriels, B. Merci, P. Demeyer, Airflow measurements in and around scale model cattle barns in a wind tunnel: Effect of ventilation opening height, Biosyst. Eng. 113 (2012) 22–32. doi:10.1016/j.biosystemseng.2012.06.003.

[10] M. De Paepe, J.G. Pieters, W.M. Cornelis, D. Gabriels, B. Merci, P. Demeyer, Airflow measurements in and around scale-model cattle barns in a wind tunnel: Effect of wind incidence angle, Biosyst. Eng. 115 (2013) 211–219. doi:10.1016/j.biosystemseng.2013.03.008.

[11] L. James Lo, D. Banks, A. Novoselac, Combined wind tunnel and CFD analysis for indoor airflow prediction of wind-driven cross ventilation, Build. Environ. 60 (2013) 12–23. doi:10.1016/j.buildenv.2012.10.022.

[12] A. Tecle, G.T. Bitsuamlak, T.E. Jiru, Wind-driven natural ventilation in a low-rise building: A Boundary Layer Wind Tunnel study, Build. Environ. 59 (2013) 275–289. doi:10.1016/j.buildenv.2012.08.026.

[13] Y. Jiang, Q. Chen, Effect of fluctuating wind direction on cross natural ventilation in buildings from large eddy simulation, Build. Environ. 37 (2002) 379–386.

[14] X. Shen, G. Zhang, B. Bjerg, Investigation of response surface methodology for modelling ventilation rate of a naturally ventilated building, Build. Environ. 54 (2012) 174–185. doi:10.1016/j.buildenv.2012.02.009.

[15] G.R. Hunt, P.P. Linden, The fluid mechanics of natural ventilation—displacement ventilation by buoyancy-driven flows assisted by wind, Build. Environ. 34 (1999) 707–720. doi:10.1016/S0360-1323(98)00053-5.

[16] A.D. Stavridou, P.E. Prinos, Natural ventilation of buildings due to buoyancy assisted by wind: Investigating cross ventilation with computational and laboratory simulation, Build. Environ. 66 (2013) 104–119. doi:10.1016/j.buildenv.2013.04.011.

[17] M. Hajdukiewicz, M. Geron, M.M. Keane, Formal calibration methodology for CFD models of naturally ventilated indoor environments, Build. Environ. 59 (2013) 290–302. doi:10.1016/j.buildenv.2012.08.027.

[18] T. Norton, J. Grant, R. Fallon, D. Sun, Optimising the ventilation configuration of naturally ventilated livestock buildings for improved indoor environmental homogeneity, Build. Environ. 45 (2010) 983–995. doi:10.1016/j.buildenv.2009.10.005.

[19] M. Samer, C. Ammon, C. Loebsin, M. Fiedler, W. Berg, P. Sanftleben, et al., Moisture balance and tracer gas technique for ventilation rates measurement and greenhouse gases and ammonia emissions quantification in naturally ventilated buildings, Build. Environ. 50 (2012) 10–20. doi:10.1016/j.buildenv.2011.10.008.

[20] M. Samer, W. Berg, M. Fiedler, C. Ammon, P. Sanftleben, R. Brunsch, Radioactive 85Kr and CO2 balance for ventilation rate measurements and gaseous emissions quantification through naturally ventilated barns, Am. Soc. Agric. Biol. Eng. 54 (2011) 1137–1148. doi:10.13031/trans.57.10572.

[21] M. Samer, C. Loebsin, M. Fiedler, C. Ammon, W. Berg, P. Sanftleben, et al., Heat balance and tracer gas technique for airflow rates measurement and gaseous emissions quantification in naturally ventilated livestock buildings, Energy Build. 43 (2011) 3718–3728. doi:10.1016/j.enbuild.2011.10.008.

[22] N.W.M. Ogink, J. Mosquera, S. Calvet, G. Zhang, Methods for measuring gas emissions from naturally ventilated livestock buildings : Developments over the last decade and perspectives for improvement, Biosyst. Eng. 116 (2013) 297–308. doi:10.1016/j.biosystemseng.2012.10.005.

[23] M.H. Sherman, Tracer-gas techniques for measuring ventilation in a single zone, Build. Environ. 25 (1990) 365–374. doi:10.1016/0360-1323(90)90010-O.

[24] S. Van Buggenhout, A. Van Brecht, S.E. Özcan, E. Vranken, W. Van Malcot, D. Berckmans, Influence of sampling positions on accuracy of tracer gas measurements in ventilated spaces, Biosyst. Eng. 104 (2009) 216–223. doi:10.1016/j.biosystemseng.2009.04.018.

[25] S. Calvet, R.S. Gates, G. Zhang, F. Estellés, N.W.M. Ogink, S. Pedersen, et al., Measuring gas emissions from livestock buildings: A review on uncertainty analysis and error sources, Biosyst. Eng. 116 (2013) 221–231. doi:10.1016/j.biosystemseng.2012.11.004.

[26] H. Takai, S. Nimmermark, T. Banhazi, T. Norton, L.D. Jacobson, S. Calvet, et al., Airborne pollutant emissions from naturally ventilated buildings: Proposed research directions, Biosyst. Eng. 116 (2013) 214–220. doi:10.1016/j.biosystemseng.2012.12.015.

[27] P. Van Overbeke, G. De Vogeleer, E. Brusselman, J.G. Pieters, P. Demeyer, Development of a reference method for airflow rate measurements through rectangular vents towards application in naturally ventilated animal houses: Part 3: Application in a test facility in the open, Comput. Electron. Agric. 115 (2015) 97–107. doi:10.1016/j.compag.2014.05.005.

[28] P. Van Overbeke, G. De Vogeleer, J.G. Pieters, P. Demeyer, Development of a reference method for airflow rate measurements through rectangular vents towards application in naturally ventilated animal houses: Part 2: Automated 3D approach, Comput. Electron. Agric. 106 (2014) 20–30. doi:10.1016/j.compag.2014.05.004.

[29] P. Van Overbeke, J.G. Pieters, G. De Vogeleer, P. Demeyer, Development of a reference method for airflow rate measurements through rectangular vents towards application in naturally ventilated animal houses: Part 1: Manual 2D approach, Comput. Electron. Agric. 106 (2014) 31–41. doi:10.1016/j.compag.2014.05.005.

[30] Y. Choinière, H. Tanaka, J.A. Munroe, A.S. -Tremblay, A wind tunnel study of the pressure distribution around sealed versus open low-rise buildings for naturally ventilated livestock housing, J. Wind Eng. Ind. Aerodyn. 51 (1994) 71–91. doi:10.1016/0167-6105(94)90078-7.

[31] R. Scholtens, C.J. Dore, B.M.R. Jones, D.S. Lee, V.R. Phillips, Measuring ammonia emission rates from livestock buildings and manure stores—part 1: development and validation of external tracer ratio, internal tracer ratio and passive flux sampling methods, Atmos. Environ. 38 (2004) 3003–3015. doi:http://dx.doi.org/10.1016/j.atmosenv.2004.02.030.

[32] Y. Choinière, J.A. Munroe, Principles for natural ventilation for warm livestock housing, in: Can. Soc. Agric. Eng., Ontario, 1990: pp. 1–17.

[33] D.W. Etheridge, Natural Ventilation of Buildings: Theory, Measurement and Design, John

Wiley & Sons Ltd, 2012. doi:10.1037/009148.

[34] ASHRAE, ASHRAE handbook: Fundamentals. Atlanta, USA, Am. Soc. Heating, Refrig. Air-Cond. Eng. (2009).

[35] L.D. Albright, Environment Control for Animals and Plants, ASABE, St. Joseph, MI, U.S.A, 1990.

[36] A. López, D.L. Valera, F. Molina-Aiz, Sonic anemometry to measure natural ventilation in greenhouses., Sensors. 11 (2011) 9820–9838. doi:10.3390/s111009820.

[37] A. López, D.L. Valera, F.D. Molina-Aiz, A. Peña, Effects of surrounding buildings on air patterns and turbulence in two naturally ventilated mediterranean greenhouses using tri-sonic anemometry, Am. Soc. Agric. Biol. Eng. 54 (2011) 1941–1950.

[38] F.D. Molina-Aiz, D.L. Valera, A. a. Peña, J. a. Gil, A. López, A study of natural ventilation in an Almería-type greenhouse with insect screens by means of tri-sonic anemometry, Biosyst. Eng. 104 (2009) 224–242. doi:10.1016/j.biosystemseng.2009.06.013.

[39] H.S. Joo, P.M. Ndegwa, a. J. Heber, B.W. Bogan, J.-Q. Ni, E.L. Cortus, et al., A direct method of measuring gaseous emissions from naturally ventilated dairy barns, Atmos. Environ. 86 (2014) 176–186. doi:10.1016/j.atmosenv.2013.12.030.

[40] M. Teitel, O. Liran, J. Tanny, M. Barak, Wind driven ventilation of a mono-span greenhouse with a rose crop and continuous screened side vents and its effect on flow patterns and microclimate, Biosyst. Eng. 101 (2008) 111–122. doi:10.1016/j.biosystemseng.2008.05.012.

[41] A. Kiwan, W. Berg, R. Brunsch, S. Özcan, H. Müller, M. Gläser, et al., Tracer gas technique , air velocity measurement and natural ventilation method for estimating ventilation rates through naturally ventilated barns, Agric Eng Int CIGR J. 14 (2012) 22–36.

[42] Y. Choiniere, J.A. Munroe, A wind tunnel study of wind direction effects on airflow patterns in naturally ventilated swine buildings, Can. Agric. Eng. (1994).

Highlights

- A naturally cross and ridge ventilated test facility was built.
- An airflow rate measuring method for side vents and ridge was developed.
- The method was successfully validated through the law of mass conservation.
- Experiments were conducted under a large range of wind incidence angles and speeds.